Solitary Waves and Fluctuations in Fragile Matter

Upadhyaya, N.

3

AMORPHOUS PACKINGS

We now consider, simple models of a disordered two dimensional packing. As a first step, we begin with a hexagonal lattice of particles that are just in contact with their nearest neighbours, but with particle masses distributed as a normal random variable. We again excite the packing with an impulse imparted to one end of the sample and follow the evolution of the excitation. Here, we find two distinct regimes of attenuation of the initial impulse excitation.

3.1 EXPONENTIAL ATTENUATION : WEAK DISORDER

For weak mass disorder (or a small variance in masses), a well defined solitary like wave is formed in response to an impulse. As the initial solitary wave propagates through the packing, it begins to attenuate and we find the initial stages of this attenuation to be well approximated as an exponential decay (see Fig. (3.3), left panel top inset).

In the last chapter, we used the quasi-particle approximation of the solitary wave to study the disintegration of a solitary wave across a mass interface [17, 39]. Consider again, an interface between two regions of sonic vacuum with grain masses m_1, m_2 respectively. For mass ratios $A = \frac{m_2}{m_1}$ close to 1, a solitary wave initially moving with amplitude P_0 is seen to split into two new solitary waves, with momentum P_1, P_2 that may be obtained using an elastic collision model that conserves the quasi-particle energy and momentum -

$$\begin{aligned} P_0 &= P_1 + P_2, \\ \frac{P_0^2}{m_{1,\text{eff}}} &= \frac{P_1^2}{m_{1,\text{eff}}} + \frac{P_2^2}{m_{2,\text{eff}}} \end{aligned} \tag{3.1a}$$

from where, we obtain

$$P_1 = \left(\frac{1-A}{1+A}\right) P_0, \tag{3.2a}$$

$$P_2 = \left(\frac{2A}{1+A}\right) P_0. \tag{3.2b}$$

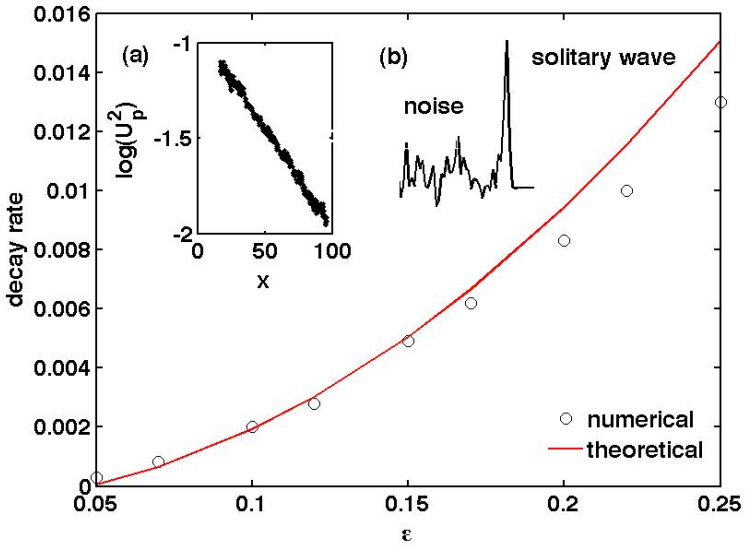

Figure 3.1: (a) The exponential decay of the solitary wave energy U_p^2 as a function of distance x along a one dimensional chain of granular particles with mass disorder modelled as a normal random variable with mean 1 and variance ϵ^2. (b) The noisy state comprising of a non-linear superposition of several smaller solitary waves left behind by the leading solitary wave as it interacts with the disorder. The main panel compares the exponent in Eq. (3.6) (solid red line) against numerical data (black circles).

Thus, the ratio of transmitted to incident energy is

$$\frac{m_{1,\mathrm{eff}}}{m_{2,\mathrm{eff}}}\frac{P_2^2}{P_0^2} \equiv \frac{T_E}{T_0} = \frac{4A}{(1+A)^2}. \tag{3.3}$$

In order to study the propagation of the solitary wave in a medium with weak mass inhomogeneity, consider a chain of beads with the mass ratio of neighbouring beads i, j related via $m_i = A_{i,j} m_j$, where $A_{i,j} = 1 + N_{i,j}(0, \epsilon^2)$, The normal random variable $N_{i,j}(0, \epsilon^2)$ has mean 0 and variance ϵ^2. Upon appealing to the localized nature of the solitary wave (its width being around 5 bead diameters and also independent of the amplitude of the solitary wave), we treat each bead as an interface and invoke the quasi-particle elastic collision model.

Thus, the energy of the leading solitary wave after the first collision is

$$\begin{aligned} T_1 &= \frac{1+\epsilon N_1(0,1)}{(1+\frac{\epsilon}{2}N_1(0,1))^2}T_0 \\ &\approx \left[(1+\epsilon N_1(0,1))\left(1-\epsilon N_1(0,1)+\frac{3}{4}\epsilon^2 N_1^2(0,1)\right)\right]T_0 \\ &\approx \left[1-\frac{1}{4}\epsilon^2 N_1^2(0,1)\right]T_0, \end{aligned}$$

where, we have retained terms up to order ϵ^2. Iterating this process $n-$ times, we find that the solitary wave energy after it has propagated n beads diameters is approximately

$$T_n \approx \left[1-\frac{1}{4}\epsilon^2 N_n^2(0,1))\cdot\cdot(1-\frac{1}{4}\epsilon^2 N_1^2(0,1)\right]T_0. \tag{3.4}$$

Retaining terms only to order ϵ^2, we find

$$\begin{aligned} \frac{T_n}{T_0} &\approx 1-\frac{1}{4}\epsilon^2\sum_{k=1}^{n}N_k^2(0,1), \\ &\approx 1-\frac{1}{4}\epsilon^2\chi^2(n), \end{aligned} \tag{3.5}$$

where, $\chi^2(n)$ is the chi function with an expectation value n. Taking the mean, we obtain that the average solitary wave energy after propagating n beads diameters reads

$$\frac{\langle T_n\rangle}{T_0} \approx 1-\frac{1}{4}n\epsilon^2 \approx e^{-\frac{n}{4}\epsilon^2}. \tag{3.6}$$

As shown in the inset to Fig. (3.3) top inset, this estimate is in very good agreement with numerical observations on an hexagonal packing and for the solitary wave attenuation in weakly-disordered granular chains [34]. Note, as the solitary wave propagates through a disordered lattice, at each subsequent collision with the material inhomogeneity, a smaller excitation in addition to a leading solitary wave is generated. This is the simplest example of how disorder effectively acts as a source of dissipation for the solitary wave, despite no source of microscopic dissipation being present in the lattice. We refer to this regime of attenuation, where the initial stages of exponential decay can be well captured, as the weakly disordered regime. Note, the reason we do not obtain an exact quantitative match in two dimensional packings is because in constructing

our quasi-one dimensional model, we are inevitably ignoring transverse degrees of motion that are necessarily excited. However, the exponential decay is in very good agreement with numerical studies on one dimensional lattices, including the prefactor $\frac{1}{4}$ for small ϵ, see Fig. (3.1) [34].

3.2 STRONG DISORDER

Our study in the previous chapter on the formation of a solitary wave train across an interface for mass ratios $A \ll 1$, provides an important prelude to the propagation of a solitary wave in a strongly disordered lattice. Consider for instance, a hexagonal lattice with masses distributed normally but with a large variance in the grain masses. Here, numerical observations reveal that an initial solitary wave (still modelled approximately by the Nesterenko solitary wave) soon transitions into a triangular shock like propagating front whose amplitude decays as a power law, while the regime of exponential decay is barely identifiable, see Fig. (3.3) middle inset.

What is the manifestation of multiple scattering by strong heterogeneity around the mechanical state of sonic vacuum ?

As may be anticipated by the formation of the solitary wave train during a collision with a strong heterogeneity, if multiple such closely located regions of strong disorder are present, multiple overlapping solitary waves will be formed. In turn, the solitary wave train will not have the occasion to separate into isolated solitary waves, since that requires a homogeneous region for them to separate asymptotically. As a result, we are only able to follow the evolution of an envelope of many such solitary waves and the spatial extent of the envelope continues to grow as more and more wave trains are generated. Eventually we find that such an envelope spans several hundred grain diameters and acquires a nearly triangular shock like profile.

The power law decay in this regime, reveals a striking similarity for the long time decay in a hexagonal packing with weak mass disorder, the dominant regime of decay in a hexagonal packing with strong mass disorder (large ϵ) as well as the dominant mechanism of decay in amorphous jammed packings, see Fig. (3.3). In all these cases, a triangular shock like profile emerges, whose leading edge decays as a power law x^{-r} with an exponent approximately $r \approx 0.5$ (solid red line). This exponent seems to be independent of the amount of disorder.

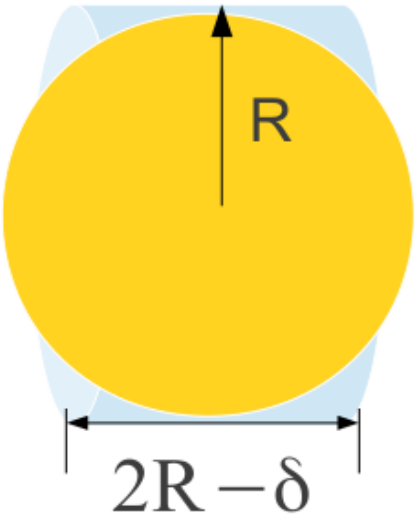

Figure 3.2: The cylindrical box around a sphere for an effective medium description. Here, R is the radius of the sphere and cylinder, while δ is the average compression.

In a recent study, the existence of very long wavelength triangular shock like fronts in a one dimensional chain of granular particles is established [43]. Here, we find that due to material inhomogeneities, an initial excitation in two dimensional disordered packings, naturally evolve into long wavelength shock solutions and their power law decay may be captured approximately (ignoring transverse excitations) from the conservation of energy [31, 43]. Below, we review the derivation of the long wavelength waves and then provide an intuitive argument for its power law decay in a disordered packing.

3.3 LONG WAVELENGTH WAVES

Here, we review the long wavelength waves that are derived for a coarse grained variable representing an averaged compressional field [43]. We first define a mass density averaged over a cylindrical segment containing a single sphere (see Fig. (3.2)):

$$\rho = \frac{m}{\pi R^2 (2R - \delta)} \tag{3.7}$$

$$\approx \frac{m}{2\pi R^3}\left(1 + \frac{\delta}{2R}\right), \tag{3.8}$$

or $\rho = \rho_0 + \rho'$, where $\rho_0 = \frac{m}{2\pi R^3}$ and $\rho' = \rho_0 \frac{\delta}{2R}$. Here, δ is the average or coarse grained compression. Defining a coarse

grained pressure p as the contact force between spheres divided by the cross-sectional area πR^2 (see Fig. (3.2)) of the chain, we find

$$p = \frac{\sqrt{2}}{3}\frac{E}{1-\nu^2}\frac{R^{1/2}}{\pi R^2}\delta^{3/2} \approx A\rho'^{\frac{3}{2}}, \tag{3.9}$$

where $A = \frac{4E}{3\pi\rho_0^{\frac{3}{2}}}(1-\nu^2)$, see Eq. (A.1)) for the prefactors. If we define v as the velocity field, the equations for mass and momentum continuity (Euler equations) are

$$\rho'_t = -(\rho v)_x, \tag{3.10}$$

$$(\rho v)_t = -\left(\rho v^2\right)_x - p_x. \tag{3.11}$$

Differentiating Eq. (3.10) once with respect to time (t), we obtain

$$\rho'_{tt} = -[(\rho v)_x]_t = -[(\rho v)_t]_x, \tag{3.12}$$

and substituting Eq. (3.11) for the last expression in the square brackets above, we find

$$\rho'_{tt} = \left(p + \rho v^2\right)_{xx} \approx A\left(\rho'^{\frac{3}{2}}\right)_{xx} + O(\rho'^{\frac{5}{2}}). \tag{3.13}$$

where, the $O(\rho'^{5/2})$ corresponds to the leading term from $\rho v^2 = \rho_0 v^2$. Recall the discussion from the introductory chapter, where for compressional shocks, the particle speeds and average compression follow a Virial like relation $v^2 \sim \delta^{\frac{5}{2}}$ (see discussion following Eq. (1.6). Consequently, if we assume the validity of this relation, then the particle speed scales as $v^2 \sim \rho'^{\frac{5}{2}}$ and is thus a higher order correction, that we ignore in Eq. (3.13). Shortly we will see that this relation is consistent with the form of the solution we obtain.

A subset of solution for Eq. (3.13) moving along the positive x- direction is (as can be verified by substituting into Eq. (3.13))

$$\rho'_t = \frac{4}{5}\sqrt{\frac{3A}{2}}\left(\rho'^{\frac{5}{4}}\right)_x = -(\rho v)_x. \tag{3.14}$$

Now, if we compare the two terms on the right (to leading order) , we find $\rho'^{\frac{5}{4}} \sim \rho_0 v$ and therefore, $v \sim \frac{\rho'^{\frac{5}{4}}}{\rho_0}$, consistent with our assumption in ignoring the term ρv^2 in Eq. (3.13).

Casting in terms of the compressional field, δ this reads

$$\delta_t = -\frac{4}{5}\sqrt{6KR^2}\left(\delta^{\frac{5}{4}}\right)_x. \tag{3.15}$$

This equation represents a coarse grained compressional field propagating along the positive x direction. Note here, the similarity with the better know inviscid Burger's equation, where the non-linear exponent is 2 instead of $\frac{5}{4}$.

3.4 SIMILARITY SOLUTION

As discussed previously in our studies, the triangular shock like fronts evolve from an initial impulse excitation irrespective of the amount of disorder. However, since our medium is in a state of sonic vacuum (no sound waves) where the only known excitations are the Nesterenko solitary waves, any other initial excitation is likely to eventually decay into a train of (possibly overlapping) solitary waves. Indeed, the long wavelength solutions first studied for one dimensional granular lattices evolve from an initially Gaussian profile.

Consequently, our investigations suggest that any initial excitation will in the long time limit evolve into a triangular shock front. This is especially true for two dimensional disordered and amorphous packings, where the disorder will ensure the attenuation of any initial solitary like wave, irrespective of the amount of disorder.

Moreover, since the dynamical response we are trying to describe is still far from any equilibrium condition, we try to look for similarity solutions to Eq. (3.15), that are often characteristic of travelling wave solutions in the regime of *intermediate asymptotics* (independent of initial condition and still far from equilibrium).

The propagating solutions we have considered elsewhere in the thesis, for instance, the steadily propagating solitary wave solutions, are also a form of similarity solution, except that they are simple translations of each other (here, the name similarity draws from similar figures in geometry that are proportional to each other but not necessarily exactly equal). Like the propagating solutions, these help reduce a partial differential equation into an ordinary differential equation. Here, the basic idea is to look for solutions of the form $f(x,t) = t^m f(\eta)$ where $\eta = xt^n$ and m, n are chosen to reduce the partial differential equation into an ordinary differential equation (in our example, x, t are taken to be space and time variables respectively, but this is not necessary).

To motivate this idea, we first start with the better know heat equation $u_t = u_{xx}$ and look for its similarity solutions by substituting $u = t^m f(\eta)$. This results in

$$mt^{m-1}f + nt^{m+n-1}xf' = t^{m+2n}f'', \tag{3.16}$$

where, primes denote derivative with respect to $\eta = xt^n$. A choice of $m = 0, n = -\frac{1}{2}$ leads to $\eta = \frac{x}{t^{\frac{1}{2}}}$ and reduces the heat equation to

$$-\frac{1}{2}\eta f' = f'', \tag{3.17}$$

which is an ordinary differential equation with a solution $f \sim \exp(-\eta^2) = \exp^{-\frac{x^2}{t}}$. Thus, we obtain the characteristic Gaussian heat kernel.

We now apply this to the non-linear equation $\delta_t + \delta^{\frac{1}{4}}\delta_x = 0$ (omitting the constant in Eq. (3.15)). Substituting $\delta = t^m f(\eta)$ leads to

$$mt^{m-1}f + nt^{m+n-1}xf' + t^{\frac{m}{4}+m+n}f'f^{\frac{1}{4}} = 0. \tag{3.18}$$

Now, a choice $m = 0, n = -1$ reduces this to an ordinary differential equation

$$-\eta f' + f^{\frac{1}{4}}f' = 0, \tag{3.19}$$

with solutions are f =constant or $f \sim \eta^4 \sim \left(\frac{x}{t}\right)^4$. This is the similarity solution describing the long wavelength shock like compressional field.

In order to connect this solution to the velocity field that we probe during simulations, we next re-cast this solution in the form of a propagating velocity field. Upon integrating once with respect to x (to obtain the displacement field from the compressional strain) and differentiating once with respect to t, we obtain the corresponding solution for the particle velocity field $\phi(x,t) \sim \left(\frac{x}{t}\right)^5$.

If we ignore the energy that goes into exciting the transverse degrees of motion (as discussed for compression shocks in Chapter 1, this is a reasonable working approximation for non-linear waves arising from strongly non-linear local interactions), the energy of the beads enclosed within the shock envelope is approximately conserved (in the longitudinal direction). Therefore,

$$E \sim \int_0^{x_f} dx\phi^2(x,t) \sim \frac{x_f^{11}}{t_f^{10}} = \text{constant}, \tag{3.20}$$

where x_f is the position of the shock front at a time t_f, see Fig. (3.3). Consequently, $t_f \sim x_f^{\frac{11}{10}}$. Thus, at the location of the shock front, the jump in the velocity field should scale as

$$\phi(x_f, t_f) \sim \frac{x_f^5}{x_f^{\frac{11}{2}}} \sim x_f^{-\frac{1}{2}}, \tag{3.21}$$

which indicates that the amplitude of front will decay as a power law with an exponent of $\frac{1}{2}$. As shown in Fig. (3.3), solid red lines, we do find this estimate to be in good agreement with the numerically determined exponent $r \approx 0.5$ for the decay of the shock front.

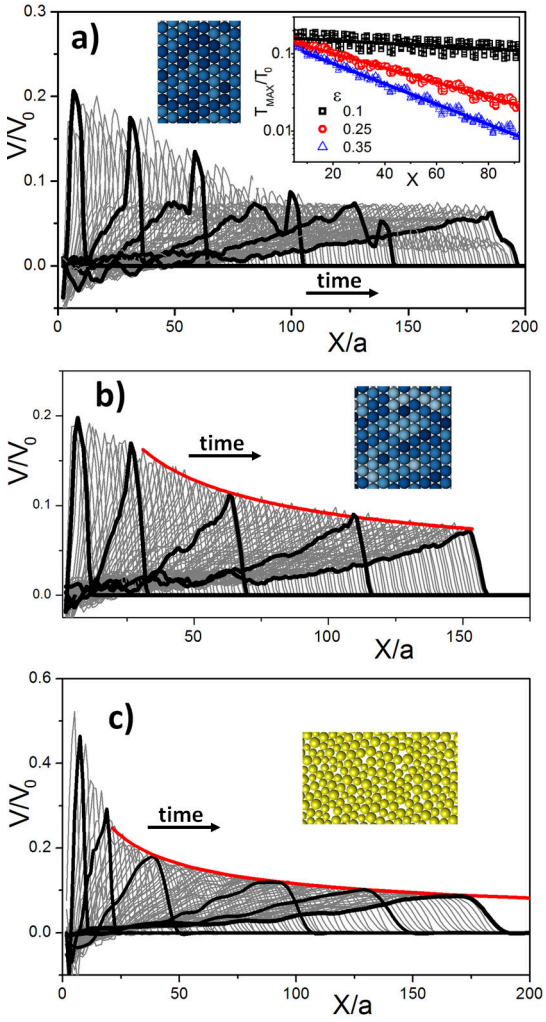

Figure 3.3: (a): The time evolution in response to an impulse in a hexagonal packing with weak mass disorder ϵ. An impulse response generates a solitary wave excitation that decays exponentially at early times. In the long time limit, a shock like triangular profile emerges whose leading edge decays as a power law with an exponent $x^{-0.5}$. (b)The time evolution in response to an impulse in a hexagonal packing with strong mass disorder ϵ. An impulse response generates a solitary wave excitation but the regime of exponential attenuation is barely identifiable. Instead, a shock like triangular profile soon emerges whose leading edge again decays as a power law with an exponent $x^{-0.5}$ (solid red line). (c) The time evolution in response to an impulse in a jammed amorphous packing prepared at a pressure of P$\sim 10^{-6}$ and an average overlap between grains $\delta_0 \sim 10^{-4}$. An impulse response still generates a solitary wave excitation but like (b), a shock like triangular profile soon emerges whose leading edge decays as a power law with an exponent $x^{-0.5}$ (solid red line).

FLUCTUATIONS AND EMERGENT HYDRODYNAMICS

Up till now, we have seen that for amorphous packings of soft frictionless disks close to their critical packing fraction, an initial impulse excitation evolves into a solitary like wave, that is progressively attenuated by disorder. For a finite size packing, what happens to the energy that was initially localized in the form of the solitary wave at very long times?

In this chapter, we demonstrate that the particle fluctuations generated by the solitary-wave decay, can be viewed as a granular analogue of temperature, that fundamentally alters the state of the packing. The presence of fluctuations leads to two emergent macroscopic properties absent in the unperturbed granular packing: a finite pressure that scales with the injected energy (akin to a granular temperature) and a wavenumber dependent viscosity that is consistent with the observations in one dimensional fluids [*].

* The research ideas presented in this chapter evolved out of discussions with V. Vitelli and L. R. Gomez and are part of Reference [45]. Thanks to L.R. Gomez for Fig 4.1.